

The millimeter and sub-millimeter rotational spectrum of triple ^{13}C -substituted ethyl cyanide[★]

A. O. Pienkina¹, L. Margulès¹, R. A. Motiyenko¹, H. S. P. Müller², and J.-C. Guillemin³

¹ Laboratoire de Physique des Lasers, Atomes, et Molécules, UMR CNRS 8523, Université de Lille I, 59655 Villeneuve d'Ascq Cedex, France
e-mail: laurent.margules@univ-lille1.fr

² I. Physikalisches Institut, Universität zu Köln, Zùlpicher Str. 77, 50937 Köln, Germany

³ Institut des Sciences Chimiques de Rennes, École Nationale Supérieure de Chimie de Rennes, CNRS, UMR 6226, 11 allée de Beaulieu, CS 50837, 35708 Rennes Cedex 7, France
e-mail: jean-claude.guillemin@ensc-rennes.fr

Received 12 December 2016 / Accepted 30 January 2017

ABSTRACT

Context. A recently published astronomical detection of all three doubly ^{13}C -substituted ethyl cyanides toward Sgr B2(N2) motivated us to investigate triple ^{13}C isotopic species that are expected to be also present in the ISM.

Aims. We aim to present an experimental study of the rotational spectrum of triple ^{13}C -substituted ethyl cyanide, $^{13}\text{CH}_3^{13}\text{CH}_2^{13}\text{CN}$, in the frequency range 150–990 GHz. We want to use the determined spectroscopic parameters for searching for $^{13}\text{CH}_3^{13}\text{CH}_2^{13}\text{CN}$ in ALMA data. The main objective of this work is to provide accurate frequency predictions to search for this molecule in the Galactic center source Sagittarius B2(N) and to facilitate its detection in space.

Methods. The laboratory rotational spectrum of $^{13}\text{CH}_3^{13}\text{CH}_2^{13}\text{CN}$ has been recorded with the Lille's fast DDS solid-state spectrometer between 150 GHz and 990 GHz.

Results. More than 4000 rotational transitions were identified in the laboratory. The quantum numbers reach $J = 115$ and $K_a = 39$. Watson's Hamiltonian in the A and S reductions were used to analyze the spectra. Accurate spectroscopic parameters were determined. The rotational spectra of the ^{13}C containing species $\text{CH}_3\text{CH}_2\text{CN}$ have been assigned, thus allowing the determination of the rotational and centrifugal distortion constants

Key words. molecular data – submillimeter: ISM – ISM: molecules – techniques: spectroscopic – line: identification – methods: laboratory: molecular

1. Introduction

Millimeter and submillimeter observations (Belloche et al. 2013, 2016) revealed that a remarkably rich chemistry occurs in the dense molecular clouds. Much of the molecular data gathered over the last 30 yr from laboratory experiments and quantum-chemical calculations have been summarized by Schoier et al. (2005). Complex organic molecules such as HCOOCH_3 (methyl formate), CH_3OCH_3 (dimethyl ether), $\text{CH}_3\text{CH}_2\text{OH}$ (ethyl alcohol), CH_2CHCN (vinyl cyanide), and $\text{CH}_3\text{CH}_2\text{CN}$ (ethyl cyanide) have been recognized in hot cores (Gibb et al. 2000a; Johnson et al. 1977) of massive star-forming regions such as Orion KL (Friedel & Widicus Weaver 2012), and Sgr B2 (Nummelin et al. 1998, 2000; Hollis et al. 2003; Müller et al. 2008).

Ethyl cyanide is an abundant molecule observed in hot molecular clouds. The core in Sgr B2, designated the Sgr B2(N) Large Molecule Heimat source or Sgr B2(N-LMH) by Snyder (2006), has the highest column densities of $\text{CH}_3\text{CH}_2\text{CN}$ of all sources studied so far ($\sim 9.6 \times 10^{16} \text{ cm}^{-2}$) (Miao et al. 1995; Kuan et al. 1996; Miao & Snyder 1997). Formation mechanisms

for $\text{CH}_3\text{CH}_2\text{CN}$ and other COMs were discussed by Laas et al. (2011), Garrod et al. (2008), Belloche et al. (2009, 2014).

The first spectroscopic detection of ethyl cyanide in Titan's atmosphere, obtained with the Atacama Large Millimeter Array (ALMA), was recently reported by Cordiner et al. (2015). $\text{CH}_3\text{CH}_2\text{CN}$ has also been observed in the coma of comet Halley (Altwegg et al. 1999), in regions of low-mass star formation (Bottinelli et al. 2007; Cazaux et al. 2003) and in high mass young stellar objects (YSOs; Bisschop et al. 2007). Observation of this molecule and its isotopologues is necessary for the comprehension of molecular cloud chemistry.

The relative natural abundance ratio of ^{13}C is about 1% of ^{12}C and is constant on the Earth. The dense clouds of the ISM contain many gas-phase organic molecules that are characterized by large deuterium enrichment compared to the terrestrial standart. Carbon fractionation is also observed and measured in ISM molecules but is less pronounced due to the smaller differential between ^{13}C and ^{12}C atomic masses. Deriving ^{13}C isotopic fractionation of the molecules by observations is one of the promising methods to constrain their main formation mechanism. The derived abundance ratios of mono-, double and triple- ^{13}C isotopologues can give suggestions about fractionation mechanisms and the origin of the fractionated carbon.

The rotational spectrum of ethyl cyanide has been measured many times in the microwave, millimeter and sub-millimeter

★ Full Table 3 is only available at the CDS via anonymous ftp to cdsarc.u-strasbg.fr (130.79.128.5) or via <http://cdsarc.u-strasbg.fr/viz-bin/qcat?J/A+A/601/A2>

ranges (Lovas 1982; Pearson et al. 1994) and (Fukuyama et al. 1996; Brauer et al. 2009; Fortman et al. 2010a,b). The rotational spectra of deuterated, mono- ^{13}C , and ^{-15}N containing isotopologs of ethyl cyanide (Margulès et al. 2009, 2016; Richard et al. 2012; Heise et al. 1974), as well as vibrationally excited ethyl cyanide (Gibb et al. 2000b; Heise et al. 1981; Mehringer et al. 2004; Daly et al. 2013; Belloche et al. 2013, 2016) have also been investigated and successfully detected in the ISM.

A recent laboratory spectroscopic investigation (Margulès et al. 2016) deals with the spectra and space identification of three double ^{13}C isotopologs studied in their ground vibrational states. However, no experimental data are available and there has been no study of the ethyl cyanide containing three ^{13}C atoms.

The present work is motivated by the relatively high abundance of ethyl cyanide in star-forming regions such as OMC-1 and Sgr B2 where other isotopologs have been observed. Our microwave studies of ethyl cyanide were extended to further isotopic species of this molecule. Since all three double- ^{13}C ethyl cyanide isotopologs have already been detected in Sgr B2, we expect that $^{13}\text{CH}_3^{13}\text{CH}_2^{13}\text{CN}$ will also be observable. The characterization of isotopologs is also important from an astronomical point of view for determining isotope abundance ratios and the observations of the denser parts of the molecular clouds. Although many isotopic varieties containing ^{13}C have been spectroscopically characterized to allow their astronomical detection (i.e., for methyl formate Carvajal et al. 2009), the ^{13}C isotopologs of many other species cannot be identified in the ISM due to their lack of spectral recordings.

Several spectroscopic investigations were performed in support of this study, for example on iso-propyl cyanide (Müller et al. 2011), anti-ethanol with one ^{13}C (Bouchez et al. 2012), 2-aminopropionitrile (Møllendal et al. 2012), and n-butyl cyanide (Ordu et al. 2012). In addition, a number of spectroscopic studies have been prompted by the results of these line surveys, for example, on methyleneaminoacetonitrile (Motiyenko et al. 2013), aminoacetonitrile (Motoki et al. 2013), and 1,2-propanediol (Bossa et al. 2014).

This paper is organized as follows. The $^{13}\text{CH}_3^{13}\text{CH}_2^{13}\text{CN}$ synthesis and spectrometer description are reported in Sect. 2. The assignment of measured transitions and obtained spectroscopic parameters are presented in Sect. 3 and conclusions are given in Sect. 4.

2. Experimental details

2.1. Synthesis

Triethylene glycol (20 mL), potassium cyanide- ^{13}C (K^{13}CN , 0.71 g, 10.7 mmol), and iodoethane- $^{13}\text{C}_2$ (1 g, 6.4 mmol) were introduced into a three-necked flask equipped with a stirring bar, a reflux condenser, and a nitrogen inlet. The mixture was heated to 110 °C and stirred at this temperature for one hour. After cooling to room temperature, the flask was fitted on a vacuum line equipped with two U-tubes. The high boiling compounds were condensed in the first trap cooled at -30 °C and propanenitrile- $^{13}\text{C}_3$ ($^{13}\text{CH}_3^{13}\text{CH}_2^{13}\text{CN}$) was selectively condensed in the second trap cooled at -90 °C. Yield: 90% based on iodoethane. The nuclear magnetic resonance data (NMR) are given in Appendix A.

2.2. Measurements with Lille's fast scan DDS spectrometer

The spectra of triple ^{13}C ethyl cyanide were recorded in the ranges 150–330, 400–660, 780–990 GHz using a fully solid-state spectrometer. The spectrometer based on the direct digital synthesizers (DDS), described in detail by Alekseev et al. (2012), was used to measure millimeter and submillimeter wave spectra of the $^{13}\text{CH}_3^{13}\text{CH}_2^{13}\text{CN}$ which is thought to be present in detectable abundances in the ISM. The Lille spectrometer provides high-precision and fast-scan measurements. This system covers the 150–990 GHz range with small gaps and uses frequency multiplier chains from VDI Inc. to multiply the frequency of the radiation generated by an Agilent synthesizer operating around 12–20 GHz. A stainless absorption cell of approximately 2 m was used. The spectrometer was equipped with a 4.2 K He cooled QMC bolometer. The measurement accuracy is estimated at 30 kHz or 50 kHz depending on the frequency range.

3. Results

Ethyl cyanide and its isotopologs are asymmetric tops. Watson's *A*-reduced Hamiltonian in the *I'* representation has been used. The rotational spectra were predicted and fit employing the SPCAT and SPFIT programs. ^{13}C isotopic substitution changes the reduced mass leading to a change in the moment of inertia and thus affecting the rotational spectrum. The $^{13}\text{CH}_3^{13}\text{CH}_2^{13}\text{CN}$ dipole moment was assumed to be unchanged upon isotopic substitution, and the values determined for ethyl cyanide given in (Kraśnicki & Kisiel 2011) of $\mu_a = 3.816$ D and $\mu_b = 1.235$ D were used.

3.1. Computational details: Theoretical prediction of the rotational spectra

Initially, $^{13}\text{CH}_3^{13}\text{CH}_2^{13}\text{CN}$ spectroscopic parameters (the ground-state rotational and the centrifugal distortion constants) have been theoretically evaluated with the Density functional theory (DFT) calculations at the B3LYP level of theory with a 6-311++g(3df, 2pd) basis set. The calculations were performed using Gaussian 09 suite of programs (Frisch et al. 2009). The theoretically optimized and experimental geometries (the bond angles, lengths and dihedrals), as well as the calculated and experimental frequencies are slightly different principally due to the use of finite basis sets, incomplete incorporation of electron correlation and the neglect of anharmonicity effects (Scott & Radom 1996). However, good agreement between the calculated and experimental frequencies can be obtained by applying scale factors.

The results of the performed DFT calculations may be sufficient to provide initial assignment of the recorded spectra. In this work, in order to obtain more accurate spectroscopic parameters for the prediction of the $^{13}\text{CH}_3^{13}\text{CH}_2^{13}\text{CN}$ rotational spectra, we used scaling factors based on the experimental data taken from the previous study of doubly ^{13}C -substituted isotopic species of ethyl cyanide (Margulès et al. 2016). We performed the following procedure. In a first step we calculated the “offsets”, that is, the differences between the theoretical and experimental values for the rotational constants *A*, *B*, *C* and centrifugal distortion constants for $^{13}\text{CH}_3\text{CH}_2^{13}\text{CN}$, $^{13}\text{CH}_3^{13}\text{CH}_2\text{CN}$ and $\text{CH}_3^{13}\text{CH}_2^{13}\text{CN}$ from Margulès et al. (2016) (Table 1). The experimental errors for all three isotopologues are close to each other, with an average of 1.925% for rotational constant *A* and less than 0.5% for *B* and *C*. Then from our theoretical rotational constants *A*, *B*, and

Table 1. An example calculation of the offset value (the difference between calculated and observed rotational constants for $^{13}\text{CH}_3\text{CH}_2^{13}\text{CN}$).

Parameter (MHz)	B3LYP/6-311G ++(3df, 2pd) ^a	Experimental data ^a	Theory-experiment =offset (MHz)	Offset/experiment ^b , %
<i>A</i>	27 840.439	27 314.27505(23)	526.16395	1.926
<i>B</i>	4556.6459	4572.983663(31)	-16.337763	-0.357
<i>C</i>	4114.3195	4112.858906(28)	1.460594	0.036

Notes. ^(a) Experimental data and DFT calculations are from Margulès et al. (2016), ^(b) experimental error.

Table 2. Determination of the rotational constants of $^{13}\text{CH}_3^{13}\text{CH}_2^{13}\text{CN}$ using the offset method which is based on the DFT calculations and previous experimental data for doubly ^{13}C -substituted isotopic species of ethyl cyanide.

Parameter (MHz)	B3LYP/6-311G ++(3df, 2pd) ^a	Scaled value ^b	Scaled value ^c	Scaled value ^d	Experimental data (this work)
<i>A</i>	27 206.198	26 680.0348	26 685.9764	26 691.67 745	26 689.77113(20)
<i>B</i>	4542.2798	4558.64176	4558.130091	4559.150643	4558.824828(34)
<i>C</i>	4088.5480	4087.06373	4085.856899	4086.646415	4086.837211(35)

Notes. ^(a) Result of the DFT calculations, this work, ^(b) from $^{13}\text{CH}_3\text{CH}_2^{13}\text{CN}$, ^(c) from $\text{CH}_3^{13}\text{CH}_2^{13}\text{CN}$, ^(d) from $^{13}\text{CH}_3^{13}\text{CH}_2\text{CN}$.

C for $^{13}\text{CH}_3^{13}\text{CH}_2^{13}\text{CN}$ isotopologue we subtracted corresponding offset values of $^{13}\text{CH}_3\text{CH}_2^{13}\text{CN}$ (Table 2). The rotational constants resulting from this computational technique are compared with the experimental values in Table 2. The agreement between offset rotational constants and experimental ones is excellent (experimental error for *A*, *B*, *C* is less than 0.05%). It is interesting to note that offsets from $^{13}\text{CH}_3^{13}\text{CH}_2\text{CN}$ proved to give a more precise determination of rotational constants and the centrifugal distortion constants among other double ^{13}C -substituted species (with an experimental error less than 0.001% for *A*, *B*, *C*). This approach provided significantly more accurate parameters and is simple and straightforward.

3.2. Assignment and analysis

Given that all three sets of rotational constants have similar accuracy, one may use any of them for initial spectral assignment. In our case we used the set of constants scaled from $^{13}\text{CH}_3^{13}\text{CH}_2\text{CN}$ isotopic species. The scaled constants allowed a very accurate calculation of rotational transition frequencies. The lines involving low K_a and $J \leq 30$ transitions were predicted to be better than 5 MHz. Thus, the offset method is very efficient for derivation of rotational constants of isotopologues when the parent species have been previously investigated.

By adding new identified transitions to the fit we cyclically improved the predictions. The analysis was strict and straightforward even given the fact that the triple ^{13}C isotopologue shows a very dense and intense spectrum. Transitions with high K_a values sometimes were difficult to assign because of weakness or line blending. Over 4000 lines have been assigned and fitted with Watson's type *A*- and *S*-reduced Hamiltonian in I' representation (Watson 1977) to a set of spectroscopic parameters. Table 4 lists all of the experimental rotational constants determined in the *A*- and *S*-reduction, and these are compared to the values from the theoretical calculations and to the experimental values of the main isotopologue from (Brauer et al. 2009). Both *A*- and *S*-reduction analyses from the present work demonstrate good similar results, with the *S*-reduction giving a slightly better rms than *A*-reduction (0.686 vs. 0.699 and 28.2 vs. 28.9) but *S*-reduction allowed to determine two additional parameters (I_4 and P_{JK}). While all spectroscopic parameters of the

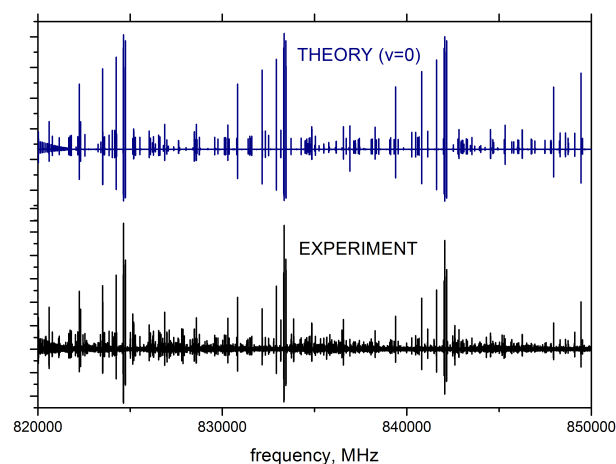


Fig. 1. Predicted (in blue) and observed (in black) rotational spectrum of $^{13}\text{CH}_3^{13}\text{CH}_2^{13}\text{CN}$ between 820 and 850 GHz. A slight inconsistency between predicted and observed spectrum, which may be visible for some strong lines, is due to source power and detector sensitivity variations.

$^{13}\text{CH}_3^{13}\text{CH}_2^{13}\text{CN}$ have been firmly determined with small relative uncertainties, some parameters were just barely determined, most notably I_{JK} and I_{KJ} . However, the values of these parameters appear to be reasonable in comparison with the corresponding values of the parent isotopic species. Figure 1 demonstrates generally good agreement between the $^{13}\text{CH}_3^{13}\text{CH}_2^{13}\text{CN}$ experimental spectra and the spectra predicted by the SPCAT program (the simulation is based upon the spectroscopic constants determined in this work). The complete list of measured rotational transitions of the ground state, presented in Table 3, is available at the CDS. Here, only a part of Table 3 is shown as an example.

4. Conclusions

Ethyl cyanide is a particularly abundant molecule in hot-core sources. In this study we have characterized the rotational spectrum of triply substituted ^{13}C ethyl cyanide for the first time. We measured and assigned about 4000 rotational lines of the $^{13}\text{CH}_3^{13}\text{CH}_2^{13}\text{CN}$ isotopologue in the frequency range from 150 to 990 GHz. The assigned lines involve rotational transitions

Table 3. Assigned rotational transitions of the ground state of $^{13}\text{CH}_3^{13}\text{CH}_2^{13}\text{CN}$.

J''	K''_a	K''_c	J'	K'_a	K'_c	Measured frequency (MHz)	Residual (MHz) A-reduction	Residual (MHz) S-reduction	Uncertainty (MHz)
38	3	36	38	2	37	200 285.7630	0.01376	0.00920	0.03000
57	4	53	57	3	54	229 870.1240	-0.04137	-0.02990	0.03000
52	5	48	52	4	49	238 942.8590	-0.04531	-0.03905	0.03000
63	4	59	63	3	60	282 864.5950	-0.02369	-0.00167	0.05000
73	3	70	72	4	69	616 550.5840	0.02133	0.01972	0.03000
91	12	80	90	12	79	785 668.5260	0.03476	0.03500	0.05000
103	8	95	102	8	94	895 732.2800	0.02518	-0.02945	0.05000
89	8	81	88	8	80	781 808.6790	-0.01659	-0.03092	0.03000
46	5	42	45	4	41	515 758.6710	0.00861	0.00848	0.03000
19	4	16	19	3	17	156 257.6970	-0.01303	-0.01426	0.03000
27	3	25	26	2	24	293 107.0420	-0.00584	-0.00657	0.03000

Notes. The full Table is available at the CDS.

Table 4. Spectroscopic parameters of triple ^{13}C isotopologue $^{13}\text{CH}_3^{13}\text{CH}_2^{13}\text{CN}$ of ethyl cyanide compared to normal species $\text{CH}_3\text{CH}_2\text{CN}$ and calculated values.

Parameter (MHz)	$\text{CH}_3\text{CH}_2\text{CN}^a$ A-Reduction	$^{13}\text{CH}_3^{13}\text{CH}_2^{13}\text{CN}^b$ A-Reduction	Parameter (MHz)	$\text{CH}_3\text{CH}_2\text{CN}^c$ S-Reduction	$^{13}\text{CH}_3^{13}\text{CH}_2^{13}\text{CN}^d$ S-Reduction
A	27 663.68306 (49)	26 689.76996(20)	A	27 663.68206 (52)	26 689.77054(19)
B	4714.213344 (76)	4558.825014(37)	B	4714.187784 (80)	4558.801153(37)
C	4235.059644 (71)	4086.837093(34)	C	4235.085063 (74)	4086.860712(34)
$\Delta_K/10^3$	548.1249 (29)	529.2239(12)	$\Delta_K/10^3$	547.7770 (29)	528.9146(12)
$\Delta_{JK}/10^3$	-47.65818(37)	-46.03111(16)	$\Delta_{JK}/10^3$	-47.26453(43)	-45.65681(16)
$\Delta_J/10^3$	3.073531 (34)	2.881015(16)	$\Delta_J/10^3$	3.008009 (37)	2.818576(16)
$\delta_J/10^3$	0.6859957 (97)	0.6528276(71)	$d_1/10^3$	-0.685888 (10)	-0.6527335(71)
$\delta_K/10^3$	12.7394 (14)	11.87496(71)	$d_2/10^3$	-0.0327755 (35)	-0.0312208(18)
$\Phi_J/10^6$	0.0103841 (66)	0.0093548(37)	$\Phi_J/10^6$	0.0093563 (74)	0.0084246(36)
$\Phi_{JK}/10^6$	-0.02512 (39)	-0.03070(19)	$\Phi_{JK}/10^6$	-0.11860 (14)	-0.114088(51)
$\Phi_{KJ}/10^6$	-1.9066 (15)	-1.83630(86)	$\Phi_{KJ}/10^6$	-1.58325 (89)	-1.54415(43)
$\Phi_K/10^6$	31.6135 (98)	30.3780(39)	$\Phi_K/10^6$	31.3192 (97)	30.1772(38)
$\phi_J/10^6$	0.0039703 (28)	0.0036282(20)	$h_1/10^6$	0.0039036 (30)	0.0035668(20)
$\phi_{JK}/10^6$	0.10144 (37)	0.08599(19)	$h_2/10^6$	0.00051409(97)	0.00046290(49)
$\phi_K/10^6$	6.501 (26)	5.590(13)	$h_3/10^6$	0.00006318(29)	0.00005988(16)
$L_J/10^{12}$	-0.05217 (55)	-0.04413(34)	$L_J/10^{12}$	-0.04237 (63)	-0.03588(34)
$L_{JK}/10^{12}$	-0.814 (25)	-0.286(15)	$L_{JK}/10^{12}$	0.522 (19)	0.5287(61)
$L_{JK}/10^9$	-0.1202 (10)	-0.00859(10)	$L_{JK}/10^9$	-0.00657 (16)	-0.004750(81)
$L_{KKJ}/10^9$	0.3986 (30)	0.09649(59)	$L_{KKJ}/10^9$	0.08327 (65)	0.07915(51)
$L_K/10^9$	-2.383 (14)	-1.9356(41)	$L_K/10^9$	-2.105 (14)	-1.9329(41)
$l_J/10^{12}$	-0.02306 (30)	-0.02003(21)	$l_1/10^{12}$	-0.02135 (32)	-0.01868(21)
$l_{JK}/10^{12}$	-0.683 (24)	-0.274(11)	$l_2/10^{12}$	-0.004351 (62)	-0.003585(29)
$l_{KJ}/10^9$	-0.0441 (17)	-0.0114(10)	$l_3/10^{12}$	-0.001170 (23)	-0.001014(13)
$l_K/10^9$	-4.378 (39)	0	$l_4/10^{12}$	-0.0001380 (86)	-0.0001016(42)
$P_J/10^{18}$	0.264 (19)	0.220(11)	$P_J/10^{18}$	0.207 (20)	0.162(11)
$P_{JK}/10^{18}$	0	0	$P_{JK}/10^{18}$	-5.12 (90)	-4.33(27)
$P_{JK}/10^{15}$	0.925 (11)	1.142(37)	$P_{JK}/10^{15}$	0.1483 (79)	0.0672(35)
$P_{KJ}/10^{15}$	0	1.911(44)	$P_{KJ}/10^{15}$	-1.707 (92)	-1.920(42)
$P_{KKJ}/10^{12}$	0	-6.33(30)	$P_{KKJ}/10^{12}$		4.26(24)
$P_K/10^{12}$	0.1424 (70)	0	$P_K/10^{12}$	0.1132 (69)	0.0
$p_J/10^{18}$	0.114 (11)	0.1050(79)	$p_1/10^{18}$	0.083 (11)	0.0809(80)
$p_K/10^{12}$	-0.0883 (37)	0	$p_K/10^{12}$	-0.0883 (37)	0
N_{lines}^b	5798	4001			4001
σ^c (kHz)	79.757	28.911		81.371	28.242
$\sigma_{\text{weighted}}^d$	0.985890	0.699187		1.001450	0.686536

Notes. ^(a) A-reduced fit from (Brauer et al. 2009), ^(b) this work, A-Reduction, ^(c) S-reduced fit from (Brauer et al. 2009), ^(d) this work, S-Reduction.

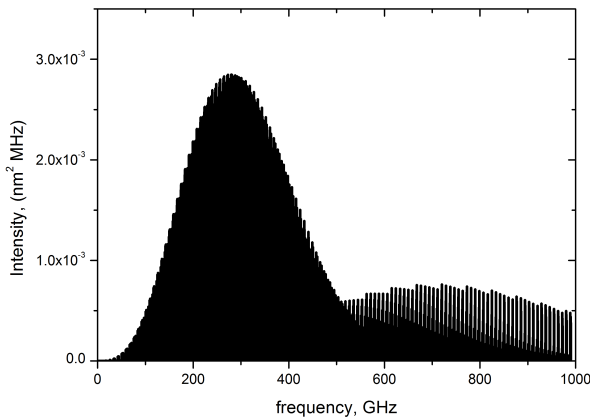


Fig. 2. Simulated spectrum of $^{13}\text{CH}_3^{13}\text{CH}_2^{13}\text{CN}$ at 150 K in the frequency range up to 1 THz.

with the rotational quantum numbers J up to 115 and K_a up to 39. The frequency range covered by direct measurements in this work corresponds to the range where the most intense lines may be observed under the characteristic temperature of 150 K in dense molecular clouds (see Fig. 2). Both A - and S -reduction Hamiltonians allow fitting all the assigned lines within experimental accuracy. The set of determined spectroscopic parameters should provide reliable predictions of the rotational transition frequencies of $^{13}\text{CH}_3^{13}\text{CH}_2^{13}\text{CN}$ up to 1.5 THz and for J and K_a quantum numbers up to 130 and 45 correspondingly.

Using the spectroscopic results of this work we searched for $^{13}\text{CH}_3^{13}\text{CH}_2^{13}\text{CN}$ in the EMoCA survey (Margulès et al. 2016) toward Sgr B2(N). We were not able to identify any isolated rotational transition of $^{13}\text{CH}_3^{13}\text{CH}_2^{13}\text{CN}$ above the detection limit in this survey. The ALMA data from the EMoCA survey suggest a column density ratio of each of the three doubly ^{13}C isotopologs to the triply substituted one of greater than eight (A. Belloche, priv. comm.). Given that we expect a $^{12}\text{C}/^{13}\text{C}$ ratio of ~ 25 , the current sensitivity is too small for the detection of the triply substituted isotopolog by at least a factor of three. Nevertheless, the present laboratory data permit to search for triply ^{13}C -substituted ethyl cyanide throughout the entire frequency region of ALMA.

Acknowledgements. This work was funded by the French ANR under the Contract No. ANR-13-BS05-0008-02 IMOLABS. This work was also supported by the French program “Physique et Chimie du Milieu Interstellaire” (PCMI) funded by the Conseil National de la Recherche Scientifique (CNRS) and Centre National d’Etudes Spatiales (CNES).

References

- Alekseev, E. A., Motiyenko, R. A., & Margules, L. 2012, *Radio Physics and Radio Astronomy*, 3, 75
- Altwegg, K., Balsiger, H., & Geiss, J. 1999, *Space Sci. Rev.*, 90, 3
- Belloche, A., Garrod, R. T., Müller, H. S. P., et al. 2009, *A&A*, 499, 215
- Belloche, A., Müller, H. S. P., Menten, K. M., Schilke, P., & Comito, C. 2013, *A&A*, 559, A47
- Belloche, A., Garrod, R. T., Müller, H. S. P., & Menten, K. M. 2014, *Science*, 345, 1584
- Belloche, A., Müller, H. S. P., Garrod, R. T., & Menten, K. M. 2016, *A&A*, 587, A91
- Bisschop, S. E., Jørgensen, J. K., van Dishoeck, E. F., & de Wachter, E. B. M. 2007, *A&A*, 465, 913

- Bossa, J.-B., Ordu, M. H., Müller, H. S. P., Lewen, F., & Schlemmer, S. 2014, *A&A*, 570, A12
- Bottinelli, S., Ceccarelli, C., Williams, J. P., & Lefloch, B. 2007, *A&A*, 463, 601
- Bouchez, A., Walters, A., Müller, H. S. P., et al. 2012, *J. Quant. Spectr. Rad. Transf.*, 113, 1148
- Brauer, C. S., Pearson, J. C., Drouin, B. J., & Yu, S. 2009, *ApJS*, 184, 133
- Carvajal, M., Margulès, L., Tercero, B., et al. 2009, *A&A*, 500, 1109
- Cazaux, S., Tielens, A. G. G. M., Ceccarelli, C., et al. 2003, *ApJ*, 593, L51
- Cordiner, M. A., Palmer, M. Y., Nixon, C. A., et al. 2015, *ApJ*, 800, L14
- Daly, A. M., Bermúdez, C., López, A., et al. 2013, *ApJ*, 768, 81
- Fortman, S. M., Medvedev, I. R., Neese, C. F., & De Lucia, F. C. 2010a, *ApJ*, 714, 476
- Fortman, S. M., Medvedev, I. R., Neese, C. F., & De Lucia, F. C. 2010b, *ApJ*, 725, 1682
- Friedel, D. N., & Widicus Weaver, S. L. 2012, *ApJS*, 201, 17
- Frisch, M., Trucks, G., Schlegel, H. B., et al. 2009, Gaussian 09, Revision A. 02 (Wallingford Inc., CT)
- Fukuyama, Y., Odashima, H., Takagi, K., & Tsunekawa, S. 1996, *ApJS*, 104, 329
- Garrod, R. T., Widicus Weaver, S. L., & Herbst, E. 2008, *ApJ*, 682, 283
- Gibb, E., Nummelin, A., Irvine, W. M., Whittet, D. C. B., & Bergman, P. 2000a, *ApJ*, 545, 309
- Gibb, E., Nummelin, A., Irvine, W. M., Whittet, D. C. B., & Bergman, P. 2000b, *ApJ*, 545, 309
- Heise, H. M., Lutz, H., & Dreizler, H. 1974, *Z. Naturforschung A*, 29, 1345
- Heise, H. M., Winther, F., & Lutz, H. 1981, *J. Mol. Spectr.*, 90, 531
- Hollis, J. M., Pedelty, J. A., Boboltz, D. A., et al. 2003, *ApJ*, 596, L235
- Johnson, D. R., Lovas, F. J., Gottlieb, C. A., et al. 1977, *ApJ*, 218, 370
- Krašnicki, A., & Kisiel, Z. 2011, *J. Mol. Spectr.*, 270, 83
- Kuan, Y.-J., Mehringer, D. M., & Snyder, L. E. 1996, *ApJ*, 459, 619
- Laas, J. C., Garrod, R. T., Herbst, E., & Widicus Weaver, S. L. 2011, *ApJ*, 728, 71
- Lovas, F. J. 1982, *J. Phys. Chem. Ref. Data*, 11, 251
- Margulès, L., Motiyenko, R., Demyk, K., et al. 2009, *A&A*, 493, 565
- Margulès, L., Belloche, A., Müller, H. S. P., et al. 2016, *A&A*, 590, A93
- Mehringer, D. M., Pearson, J. C., Keene, J., & Phillips, T. G. 2004, *ApJ*, 608, 306
- Miao, Y., & Snyder, L. E. 1997, *ApJ*, 480, L67
- Miao, Y., Mehringer, D. M., Kuan, Y.-J., & Snyder, L. E. 1995, *ApJ*, 445, L59
- Møllendal, H., Margulès, L., Belloche, A., et al. 2012, *A&A*, 538, A51
- Motiyenko, R. A., Margulès, L., & Guillemin, J.-C. 2013, *A&A*, 559, A44
- Motoki, Y., Tsunoda, Y., Ozeki, H., & Kobayashi, K. 2013, *ApJS*, 209, 23
- Müller, H. S. P., Belloche, A., Menten, K. M., Comito, C., & Schilke, P. 2008, *J. Mol. Spectr.*, 251, 319
- Müller, H. S. P., Coutens, A., Walters, A., Grabow, J.-U., & Schlemmer, S. 2011, *J. Mol. Spectr.*, 267, 100
- Nummelin, A., Bergman, P., Hjalmarson, Å., et al. 1998, *ApJS*, 117, 427
- Nummelin, A., Bergman, P., Hjalmarson, Å., et al. 2000, *ApJS*, 128, 213
- Ordu, M. H., Müller, H. S. P., Walters, A., et al. 2012, *A&A*, 541, A121
- Pearson, J. C., Sastry, K. V. L. N., Herbst, E., & De Lucia, F. C. 1994, *ApJS*, 93, 589
- Richard, C., Margulès, L., Motiyenko, R. A., & Guillemin, J.-C. 2012, *A&A*, 543, A135
- Schoier, F. L., van der Tak, F. F. S., van Dishoeck, E. F., & Black, J. H. 2005, *A&A*, 432, 369
- Scott, A. P., & Radom, L. 1996, *J. Phys. Chem.*, 100, 16502
- Snyder, L. E. 2006, *Proc. Natl. Acad. Sci. USA*, 103, 12243

Appendix A: Propanenitrile- $^{13}\text{C}_3$

^1H NMR (CDCl_3 , 400 MHz) δ 1.29 (dddd, $^1J_{\text{CH}} = 126.1$ Hz, $^3J_{\text{CH}} = 6.6$ Hz, $^2J_{\text{CH}} = 4.6$ Hz, $^3J_{\text{HH}} = 7.7$ Hz, CH_3), 2.35 (tdq, 2H, $^1J_{\text{CH}} = 135.0$ Hz, $^2J_{\text{CH}} = 9.7$ Hz, $^3J_{\text{HH}} = 7.7$ Hz, CH_2). ^{13}C NMR (CDCl_3 , 100 MHz) δ 10.5 (ddq, $^1J_{\text{CC}} = 33.5$ Hz, $^2J_{\text{CC}} = 4.4$ Hz, $^1J_{\text{CH}} = 126.1$ Hz, CH_3), 11.1 (ddt, $^1J_{\text{CC}} = 48.7$ Hz, $^1J_{\text{CC}} = 33.5$ Hz, $^1J_{\text{CH}} = 135.0$ Hz, CH_2); 120.8 (dd, $^1J_{\text{CC}} = 48.7$ Hz, $^2J_{\text{CC}} = 4.4$ Hz, CN).